Journal of Environmental Chemical Engineering 5 (2017) 5868–5875

Contents lists available at ScienceDirect

Journal of Environmental Chemical Engineering

journal homepage: www.elsevier.com/locate/jece

Research paper

Montmorillonite-alginate beads: Natural mineral and biopolymers based sorbent of paraquat herbicides

Mariana Etcheverry[a], Valeria Cappa[b], Jorge Trelles[b], Graciela Zanini[a,*]

[a] INQUISUR, Departamento de Química, Universidad Nacional del Sur (UNS)-CONICET, Av. Alem 1253, (8000) Bahía Blanca, Argentina
[b] Laboratorio de Investigación en Biotecnología Sustentable (LIBioS), Departamento de Ciencia y Tecnología de la Universidad Nacional de Quilmes, Roque Sáenz Peña 352, B1876BXD Bernal, Buenos Aires, Argentina

ARTICLE INFO

Keywords:
Montmorillonite
Alginate
Beads
Adsorption
Paraquat

ABSTRACT

Beads of alginate montmorillonite have been used for the first time as sorbent of the cationic pesticide paraquat (PQ). They are a green material because they are formed by a biopolymer and a clay mineral, and because they allow using an energy efficient process to separate the beads after PQ adsorption. The general characterization of the beads, with montmorillonite contents ranging from 0% to 70%, has been carried out by elemental composition, FTIR and thermal analysis. The shape, external morphology and internal structure of the beads were examined by SEM. Wet beads were also observed with a digital camera. PQ adsorption was studied with adsorption isotherms from aqueous solutions, and maximum adsorption capacities (Q_{max}) were 0.093, 0.146, 0.187 and 0.278 mmol g^{-1} for montmorillonite contents of 0, 5, 30 and 70%, respectively. Q_{max} varied linearly with the clay content. The results show that montmorillonite is practically the only PQ sorbent, with alginate acting mainly as support of the clay particles, but playing a very important role allowing an effortless handling of the material and the adsorbed pollutant.

1. Introduction

Herbicides are continuously used to minimize the loss of crop productivity, but more than 99.9% of the applied pesticides move into the environment where they can adversely affect beneficial biota and contaminate soil, water, and the atmosphere [1]. Paraquat dichloride (PQ; 1,1-dimethyl-4,4-bipyridium dichloride) is a toxic quaternary ammonium herbicide and is widely used in agriculture as a non-selective agent for controlling broadleaf [2]. Introduced in the 1960s, PQ has now been banned in some countries because of its toxicity [3,4]. However, it is used in USA and several countries of South America, Australia, Asia, etc., which still permit that this agent to be used for example in chemical desiccation [5], controlling weeds in broad-acre cropping[6,7], rice field crops [8], etc.

The LD50 of PQ in humans is approximately 3–5 mg/kg, which translates into as little as 10–15 mL of a 20% solution. If PQ has been ingested in any amount it is necessary immediately administer an adsorbent. A clay suspension as Bentonite (7.5%) is highly effective [9].

Various techniques are being used to remove pollutants from aqueous waste [10,11], with sorption being one of the most promising technologies for water purification. The most widely used adsorbents in this concern include clay minerals [12], activated carbon [13] and polymers [14,15]. Thus, there is a growing interest in the use of bio-based materials such as polymers obtained from natural resources due to their environmentally friendly properties and renewable abundance [16–18].

The adsorption studies of PQ on materials easy to handle and nontoxic are important for cleaning water and as a therapeutic measure in case of intoxication. Alginate beads are a well-known support material in bioscience application [19] for immobilization of enzymes [20] and living cells [21]. Over the past few years they are being used in the environmental field for the removal of some heavy metal ions and organic pollutants [22–25]. The capacity of alginate to form gel in the presence of multivalent cations (ionotropic gelation technique) has been exploited to prepare multiparticulate systems, incorporating numerous drugs, proteins, cells or enzymes. Alginates are polysaccharides derived mainly from brown seaweed. Sodium alginate is the water soluble form, that upon quenching with Ca^{2+} crosslinks to the water insoluble form of calcium alginate. The divalent cation bridges the gap between two polymer chains, in turn stabilizing the network. This material, calcium alginate, is biocompatible, biodegradable, immunogenic, non-toxic, economical and can be easily prepared [26]. Alginate beads face problems such as distorted shapes, uneven sizes, poor mechanical strength and high porosity [27]. To improve the

* Corresponding author.
E-mail address: gzanini@uns.edu.ar (G. Zanini).

https://doi.org/10.1016/j.jece.2017.11.018
Received 27 May 2017; Received in revised form 13 October 2017; Accepted 4 November 2017
Available online 08 November 2017

properties of the beads, alginate can be loaded with montmorillonite clay [28]. Montmorillonite is a layered structure consisting of a sandwich of one octahedral alumina sheet between two tetrahedral silica sheets [29]. Fortunately, this clay not only improves the mechanical properties of the beads, but also the adsorptive properties. The montmorillonite (natural or modified) has been used for more than 40 years for the removal of toxic metals or organic pollutants [30–33] from aqueous solutions. This inorganic solid has favourable surface properties, availability, environmental and economic considerations. The specific properties of montmorillonite are its high cation exchange capacity, adsorption, high surface area and swelling behaviour [34].

In recent years, clays supported on calcium alginate beads have been reported to improve the mechanical and thermal stabilities of the beads and also to simplify the separation procedures compared to the use of natural clays [35]. The most interest in studies for the use of alginate-clays beads as adsorbents has been for the removal of dyes from aqueous solutions [36–38] or for controlled release of difference substances [39,40]. However, there are insufficient studies for the use of these kinds of materials to adsorb pesticides for cleaning or decontamination. In the particular case of PQ, montmorillonite has been used in several reports as the adsorbent [41,42], but there is not information regarding alginate-montmorillonite beads as adsorbent of PQ. Besides, it is unknown if the montmorillonite forming the bead adsorbs PQ in the same way that the montmorillonite in powder does. The possibility to use these beads instead of the powdered clay to remove pesticides would really be a significant improvement of remediation technologies using adsorption process. The use of these materials would help during the separation process because it is not necessary to wait a long time for sedimentation after adsorption, as it occurs with clays [43]. Centrifugation will not be necessary either because after shaking and due to gravity, the alginate-montmorillonite beads are deposited at the bottom of the reactor.

In this report we present the synthesis and characterization of alginate beads with different contents of montmorillonite. The aim is to study the adsorption of PQ onto these alginate-montmorillonite beads from aqueous solutions and to assess how the clay content affects the adsorption. The role played by alginate and montmorillonite in the beads is investigated and highlighted.

2. Experimental

2.1. Materials and reagents

Sodium alginate was obtained from Fluka (Switzerland, N° 71238), Mw = 231,500 g/mol) Na-Montmorillonite (99.4% purity) was obtained from Lago Pellegrini (Rio Negro, Argentina). Paraquat (99%) was supplied by Supelco (molecular structure shown in Scheme 1) and calcium chloride ($CaCl_2$) was supplied by Sigma-Aldrich Company.

2.2. Synthesis and characterization of alginate-montmorillonite beads

A 1% (w/v) Na-alginate solution was prepared by solving 1 g of sodium alginate into 100 mL distilled water at room temperature. Then, different amounts of montmorillonite (MMT) were added to the gel with continuous stirring (0.1; 1.0 and 4.0 g) obtaining suspensions of

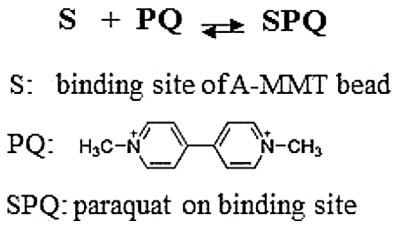

Scheme 1. Describes in a general way the adsorption reaction of PQ onto A-MMT beads.

Table 1
Sample description.

Alginate suspension (%)	MMT suspension (%)	MMT content per gram of bead (%)[a]	Denomination
1	0	0	**A-MMT0**
1	0.1	5	**A-MMT5**
1	1	30	**A-MMT30**
1	4	70	**A-MMT70**

[a] The MMT content per gram of bead was estimated from elemental analysis shown in Section 3.1.

0.1; 1 and 4% (w/v) of MMT. Once the mixture was homogeneous it was forced through a micropipette tip by a peristaltic pump. The resulting gel droplets were collected in a stirred reservoir containing 0.1 M $CaCl_2$ solution. The beads were allowed to harden in this solution for few minutes. Afterwards hard spherical beads containing the MMT were obtained. The beads were filtered and rinsed several times with distilled water to remove calcium chloride from its surface. They were then stored in NaCl 0.1 M until use. When calcium alginate beads were used as a blank, the same procedure as before was followed, but in this case there was no addition of MMT.

The beads will be named as **A-MMT0**; **A-MMT5**; **A-MMT30** and **A-MMT70** as is shown in Table 1.

2.3. Characterization

Exeter Analytical, INC, model CE440 Elemental Analysis instrument was employed in the performance of the elemental analysis of the alginate and alginate-montmorillonite beads. The wet beads were observed with a D5100 Nikon Digital camera. The shape, external morphology and internal structure of the beads were examined by scanning electron microscopy (SEM). Images (at different magnifications) of dry whole beads and their cross sections were captured on an LEO microscope model EVO 40. The samples were exposed to an accelerated voltage beam strength of 10.0 KV.

The thermogravimetric analysis (TGA) was performed with the STD Q600 of TA Instruments operated in air. The 25 μg powder samples in a ceramic crucible were heated in air from 20 °C to 1000 °C at the rate 10 °C/min. The maximum variability between two replicates was 0.2% on a mass basis. The maximum degradation temperature was determined with a precision of ± 3 °C.

The crystallinity and structure of the dried materials were examined by XRD on a Rigaku D-Max III – C equipped with a Cu $K_{\alpha 1}$ (λ = 1.54059 Å) radiation and graphite monochromator operated at 35 kV and 15 mA over the 2θ range of 3–80° and 25 °C at a scan rate of 0.02° s^{-1}. The XRD patterns are presented in the Supplementary material.

The FTIR spectra of the samples were recorded using KBr pellets on a Nicolet Nexus 470 FTIR spectrometer equipped with a DTGS detector over a range of 4000–400 cm^{-1}.

The N_2 adsorption-desorption isotherms at 77 K (BET) were performed with a Micromeritics – ASAP 2000 instrument. Prior to the measurements, the dried samples were outgassed for at least 12 h at 333 K.

Electrophoretic mobilities of sodium alginate, MMT, A-MMT0, A-MMT70 and A-MMT70 with PQ adsorbed (PQ_{ads} A-MMT70) at different pH and in 0.01 M NaCl were determined with a Malvern Nano ZS90 equipment. The experiments were carried out at 25.0 °C. Zeta potential (ζ) data were automatically calculated with the Smoluchowski equation by the equipment. It was necessary to dry the beads, grain them and prepare the suspensions in 0.01 M NaCl. Although this preparation changed the appearance of the beads, the information obtained was useful. The concentration of the solid was 0.1 g L^{-1} for MMT, A-MMT0, A-MMT70 and PQ_{ads} A-MMT70 and 1 g L^{-1} for sodium alginate.

2.4. Adsorption experiments

Adsorption isotherms were obtained by performing batch adsorption experiments. Four alginate-clay beads were placed in 15 mL polycarbonate centrifuge tubes. After that proper volumes of 0.01 M NaCl and appropriate aliquots of stock solution of paraquat were added to cover concentration ranges from 5.0×10^{-5} to 3.0×10^{-3} M. The final volume in each tube was 10 mL. The pH was 5.5 ± 0.2 in all experiments. The tubes were shaken end-to-end for 6 h. Kinetic experiments showed that 6 h of equilibration time was enough to obtain an equilibrium condition between adsorbent and adsorbate. The kinetics data are shown in the Supplementary material. All experiments were carried out at room temperature (25 ± 1 °C) and 0.01 M NaCl ionic strength. Adsorption studies were also carried out using alginate beads without MMT and with a suspension of MMT without alginate. After shaking, all the beads settled in the bottom of the tube and they were easily separated leaving a clear supernatant (Supplementary material). In all PQ adsorption experiments, the pH was checked before and after adsorption, and no changes were detected (only a random variation of 0.1 pH unit).

PQ concentrations remaining in the supernatants were spectrophotometrically measured by recording the UV/vis spectra in the 200–800 wavelength range and the absorbance was controlled at 257 nm. Spectrophotometric quantifications were done with an Agilent 8453 diode-array UV/vis spectrometer using a 1 cm quartz cell.

The adsorbed amount of PQ (Q_{ads}, in mmol g^{-1}) was calculated according to the following equation:

$$Q_{ads} = (C_0 - C_{eq})V/W \quad (1)$$

where C_0 and C_{eq} (mM) are the initial and equilibrium concentration of PQ respectively; V is the volume of the solution in L; and W is the weight of the dry beads in g.

3. Results and discussion

3.1. Characterization of beads

3.1.1. Elemental analysis of alginate and alginate-montmorillonite beads

The results obtained from the elemental analysis are collected in Table 2. The carbon content (%C) comes from alginate. Then from %C the clay content was estimated (%MMT). It is clear by comparing Tables 1 and 2 that increasing MMT content results in a decrease in alginate content.

3.1.2. Digital photography and SEM

Fig. 1 shows the digital photograph. As can be seen they are spherical in shape and the size is not significantly influenced by the clay content, while the transparency is reduced upon the addition of the clay mineral amount. The introduction of MMT into alginate beads was accompanied by a significant change in colour, from uncoloured to white, and easily detectable by the naked eye. The diameter average of the wet beads was 3.0 ± 0.10 mm. The formation of alginate beads with clays, such as reported in literature, could be driven by polar interactions between the uncharged siloxane moieties of the clay and the hydroxyl groups of the alginate biopolymer [35].

Fig. 2 shows the SEM micrographs of dried beads and MMT. The dried beads resulted to be spherical with an average diameter of 1000 μm (Fig. 2a) with the surface different for each condition. The surface morphology of dry powder of montmorillonite in Fig. 2b, shows a typical expanded, flared, “cornflake” texture of the clay [44]. It is clear from Fig. 2b that the surface of MMT has an aggregated and foliated appearance due to the presence of the layered structure [45]. Looking at the SEM micrograph, the presence of clay could easily be detected within the beads. Figs. 3 and 4 show the morphology surface and interphase beads, respectively. The surface morphology shows that the surface of most of them is similar to the surface of alginate beads without clay, but as the amount of clay increases the surface loses uniformity. The morphology interphase shows that as the amount of montmorillonite increase the clay folds can be seen more clearly indicating the presence of the MMT inside the beads.

Table 2
Elemental analysis of the beads.

Sample	%C	%H	%N
A-MMT0	16.505	3.381	0.077
A-MMT5	15.760	3.137	0.010
A-MMT30	11.160	2.605	0.046
A-MMT70	4.407	2.100	0.010

3.1.3. XRD diffraction and BET specific surface area

The XRD patterns of the MMT and A-MMT70 beads are presented in Supplementary material. Montmorillonite revealed its characteristic peak at 2θ = 7.16°, which corresponds to a d-spacing of 1.23 nm [46]. The presence of alginate practically did not affect the basal spacing of the clay, indicating that alginate was unable to intercalate between the silicate layers.

The specific surface areas are for A-MMT0; A-MMT70 and MMT were 1; 33 and 46 $m^2\,g^{-1}$, respectively. For montmorillonite, N_2 can cover the outer primary surface area, but not the interlayer space, as indicated by small surface areas measured by this method. It is important to note that the informed areas of A-MMT0; A-MMT70 correspond to the dried beads.

3.1.4. Infrared spectroscopy

Fig. 5 shows the FT-IR spectra of calcium alginate beads (Fig. 5a), MMT (Fig. 5b) and alginate-montmorillonite beads (A-MMT70) (Fig. 5c).

Alginate characteristics bands have been widely described in the literature [47–49]. At 3410 cm^{-1} a broad band corresponding to stretch vibration of hydroxyl groups (ν_{O-H}) is observed. The vibration of Csp^3–H bond appears at 2920 cm^{-1}. Two strong peaks at 1610 and 1420 cm^{-1} are attributed to the asymmetric and symmetric stretching of carboxyl groups ($\nu^{as}_{COO^-}$; $\nu^{s}_{COO^-}$), respectively. The signals observed in the range of ~ 1170–1030 cm^{-1} correspond to symmetric and asymmetric vibration bands of C—O—C bonds (ν^{s}_{C-O-C}; ν^{as}_{C-O-C}) typical of polysaccharide rings [50].

Fig. 5b shows the characteristic peaks for MMT, at 3630 cm^{-1} corresponding to the hydroxyl stretching of Si—OH. A broad band centred at 3440 cm^{-1} due to –OH symmetric stretching for interlayer adsorbed water [51,52] and the hydroxyl bending of water at 1640 cm^{-1} [53]. An intense band was observed at 1040 cm^{-1} assigned to the asymmetric stretching vibrations of Si—O—Si [53,54]. Another band at 918 cm^{-1} corresponds to the hydroxyl bending vibrations that suggests that the Al^{3+} ions occupy octahedral sites [55,56]. Finally the bending vibrations of Si—O—Al at 523 cm^{-1} and Si—O—Si at 465 cm^{-1} corresponded [53,54,57] (Fig. 5b).

Fig. 5c shows the A-MMT70 spectrum. This sample contains 70% of MMT and 30% of alginate and it is easy to observe that the spectrum is a mix of alginate and montmorillonite spectrum.

3.1.5. Thermal analyses (TGA)

TGA was used to determine the thermal stability of the beads.

In general, the thermal decomposition of polysaccharides follows three stages. Stage one includes the desorption of physically absorbed water and removal of structural water at temperature range between 40 and 160 °C [58]. Stage two with temperatures around 250–350 °C includes the depolymerisation (accompanied by the rupture of C—O and C—C bonds in the ring units resulting in the formation CO, CO_2 and H_2O). Finally at around 550 °C a third stage involves the decomposition of carbonized products [59–61]. Soares et al. [62], presented at TGA

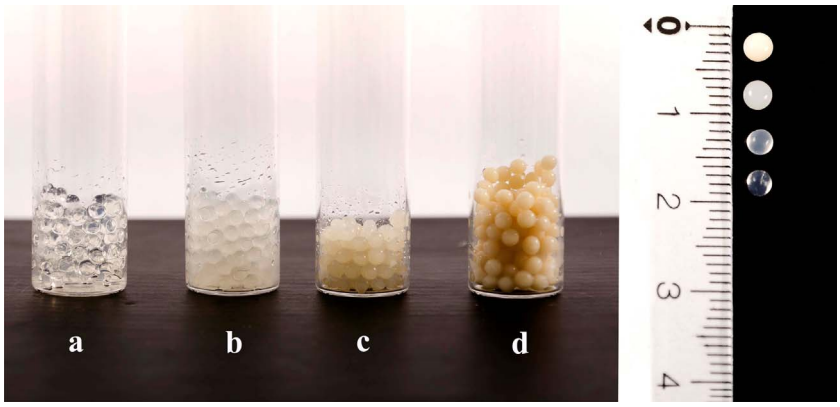

Fig. 1. Optical images for beads at variable montmorillonite content: a) A-MMT0; b) A-MMT5; c) A-MMT30 and d) A-MMT70. The scale is in cm.

study for the sodium alginate salt. Besides of water loss around 25–150 °C, the authors observed that the salt decomposed by degradation from 200 to 600 °C to sodium carbonate and a carbonized material that decomposes slowly from 600 to 750 °C in N_2. They found similar results under air. They also evidenced with DSC an endothermic peak close to 100 °C attributed to the water release and the decomposition of the carbonaceous material represented for exothermic peaks above 300 °C.

The thermal behaviour of MMT shows two distinct steps: the first one, around 100 °C, is due to the loss of free water, and the second, around 650 °C, is due to the loss of structural OH [63]. It is known that both observed processes are endothermic [64].

The characteristic weight losses of alginate and montmorillonite appear in the studied alginate-montmorillonite beads, as shown in Fig. 6. All beads present an initial weight loss up to 150 °C, corresponding to dehydration. Regarding the other processes, DTG curves show that the thermal behaviour of the beads progressively changes from the behaviour of pure alginate (sample A-MMT0) to the behaviour of MMT as the clay content increases. The DSC curves (Supplementary material) show the characteristic endothermic peaks due to loss of free water in all samples. MMT presents its endothermic peak around 650 °C, and all beads present exothermic peaks due to decomposition of alginate.

The residues of the samples A-MMT0; A-MMT5; A-MMT30; and A-MMT70 and MMT after heating at 1000 °C were 19.66; 35.79; 50.19; 67.97 and 84.15% of the initial mass, respectively. These residues show that A-MMT beads in all conditions present an improvement of thermal stability compared with alginate beads A-MMT0.

3.2. Adsorption isotherms

Adsorption isotherm is important in describing the relationship between the adsorbate and adsorption. The study of adsorption isotherms requires that the system reaches equilibrium, for that it is important to make a prior kinetic study. The figure of this study is shown in the Supplementary material.

Fig. 7a shows the adsorption isotherm of PQ onto the beads at pH 5.5 (A-MMT0; A-MMT5; A-MMT30 and A-MMT70) and the MMT suspension. Isotherms data were fitted with the Langmuir model and the PQ adsorption isotherm parameters on the beads are presented in Table 3. This model can be described by the following equation:

$$Q_{ads} = Q_{\max} K_L C_{eq} / (1 + K_L C_{eq}) \quad (2)$$

where Q_{ads} is the amount of solute adsorbed (mmol g^{-1}), C_{eq} is the equilibrium concentration of adsorbate (mM); Q_{max} (mmol g^{-1}) and K_L (L $mmol^{-1}$) are the Langmuir parameters that represent respectively the maximum amount of PQ adsorbed and the Langmuir constant, which is related to the affinity of PQ for the beads.

Fig. 7 shows that as the amount of clay in the beads is increased, the PQ adsorption isotherms start taking the shape of the isotherm of PQ adsorbed on montmorillonite. Table 3 shows the Langmuir fit parameters. The values of K_L and Q_{max} increase by increasing the amount of MMT indicating that the PQ affinity for bead and the maximum amount of pesticide adsorbed on the bead is greater as the amount of clay increases. It can be said that the pesticide is adsorbed onto the beads with 0% and 5% MMT with less affinity than beads containing 30% and 70% of MMT. These results can be explained because it is known that PQ can be adsorbed to the montmorillonite with high affinity through a cation exchange mechanism and Q_{max} reaches the clay CEC values [33,41].

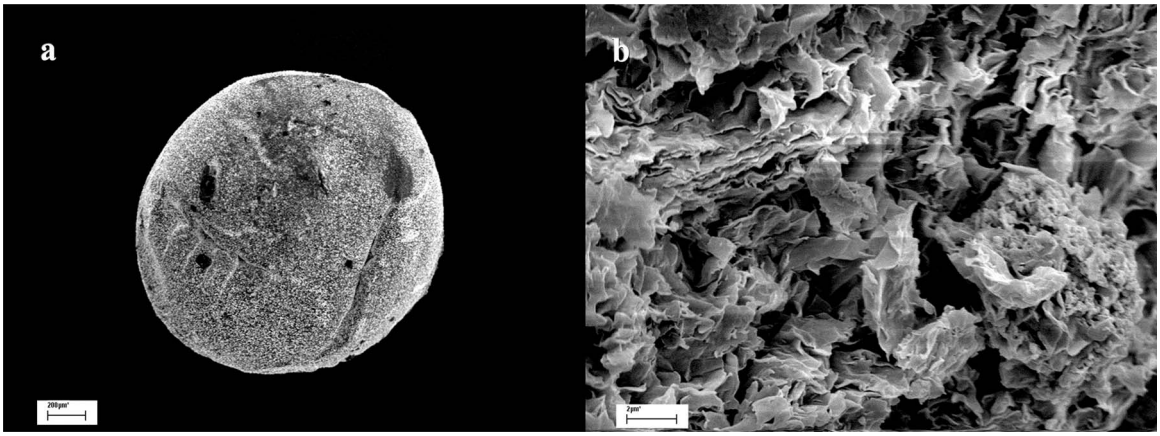

Fig. 2. SEM micrographs of a) dried beads at 100×; scale: 200 μm^2 and b) MMT at 13400×; scale: 2 μm^2.

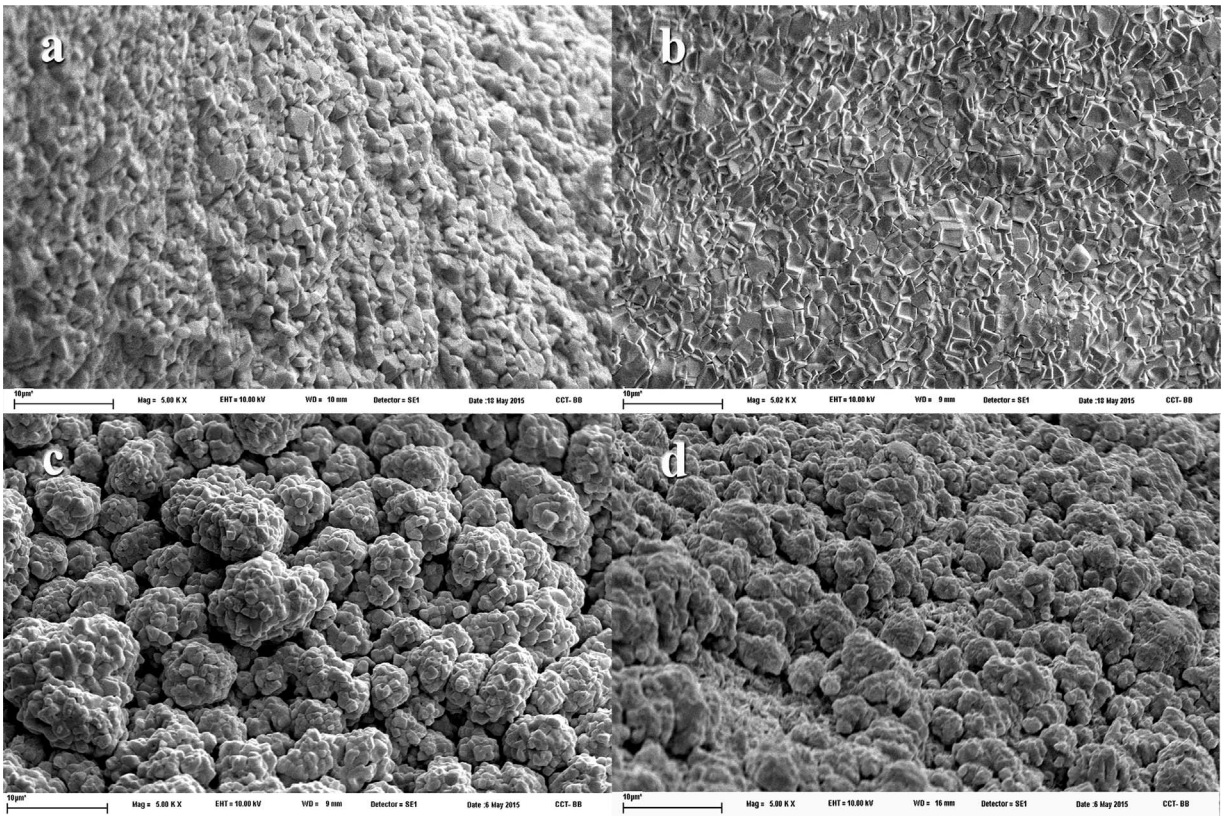

Fig. 3. SEM micrographs of surface morphology beads at 5000×; scale: 10 μm^2 a) A-MMT0; b) A-MMT5; c) A-MMT30 and d) A-MMT70.

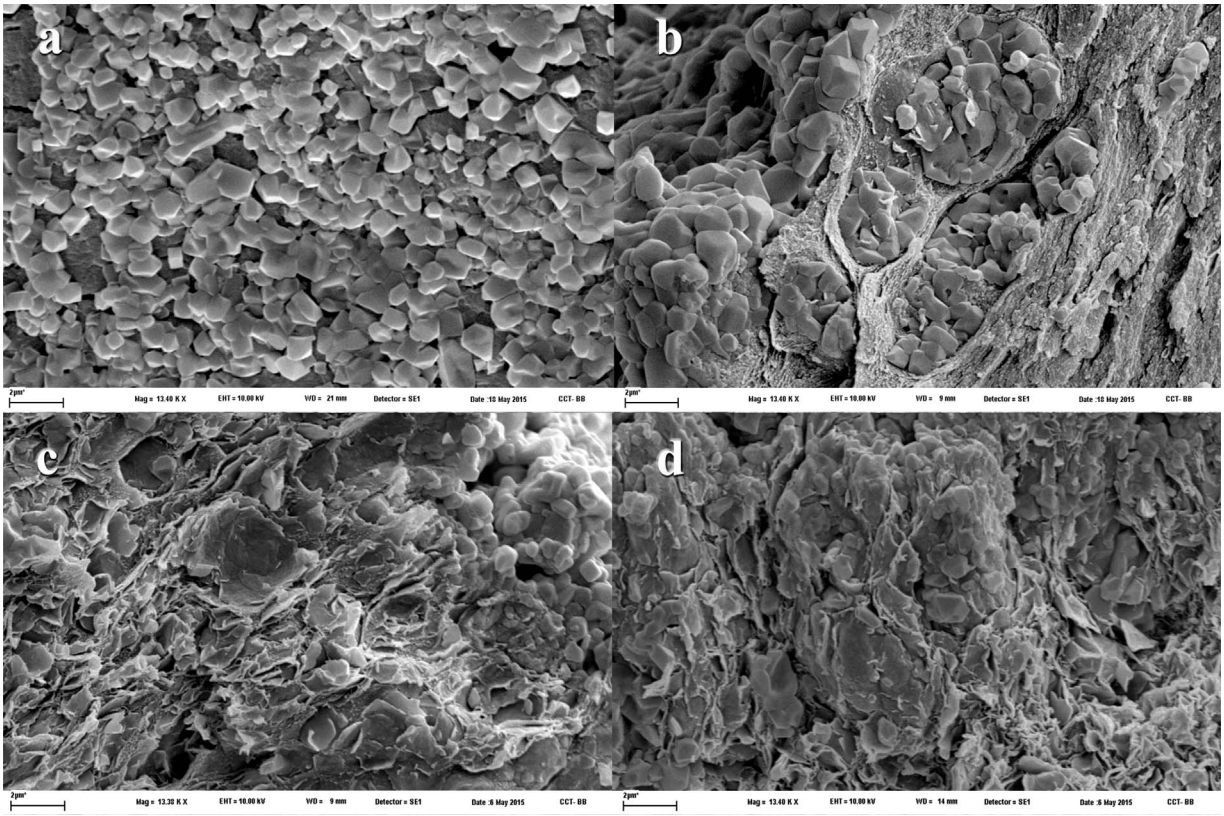

Fig. 4. SEM micrographs of interphase beads at 13000×; scale: 2 μm^2 a) A-MMT0; b) A-MMT5; c) A-MMT30 and d) A-MMT70.

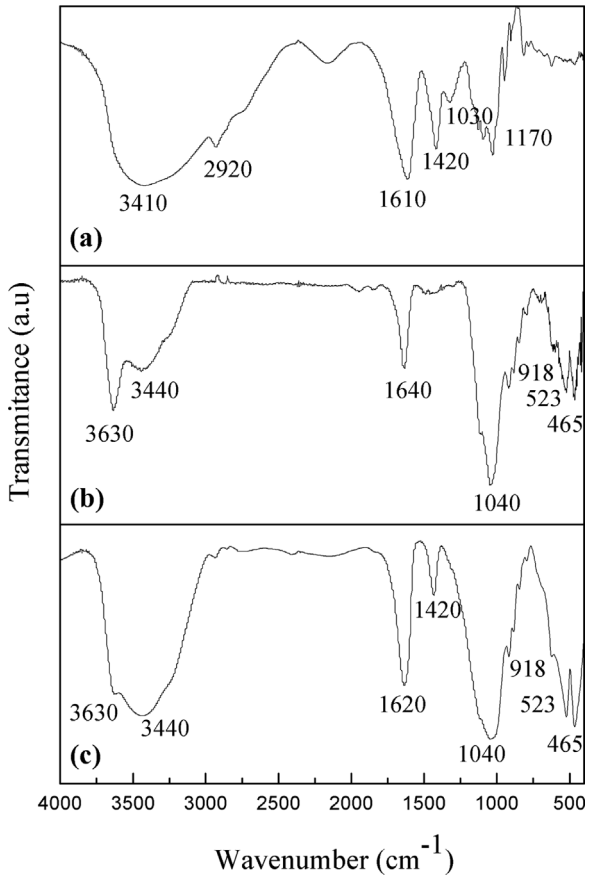

Fig. 5. FT-IR spectra of: a) calcium alginate beads; b) montmorillonite; and b) alginate-montmorillonite beads.

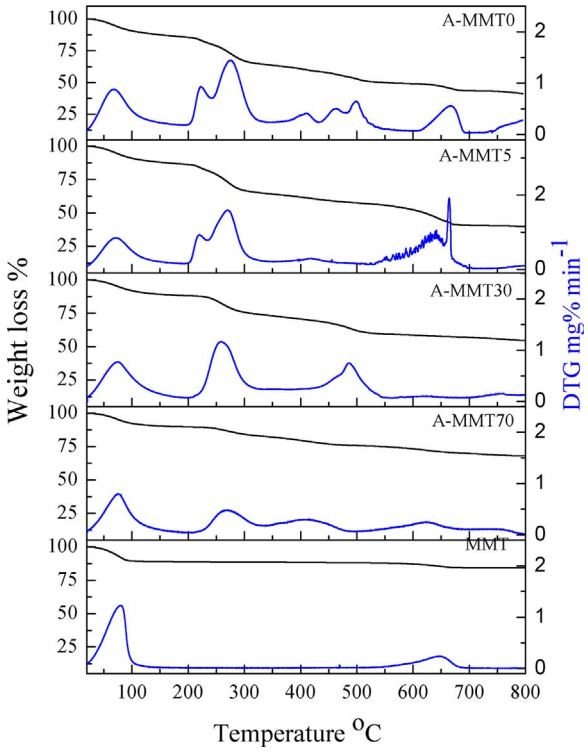

Fig. 6. TGA (black lines) y DTG (blue lines) curves of A-MMT beads and MMT heated at 10 °C/min up to 1000 °C. MMT; b) A-MMT0 c) A-MMT5; d) A-MMT30 and e) A-MMT70. The identification of endothermic and exothermic peaks is given in DSC curves in Supplementary material. (For interpretation of the references to colour in this figure legend, the reader is referred to the web version of this article.)

Fig. 7 shows that a small amount of PQ is adsorbed on the alginate beads without clay (A-MMT0). The polymer also has negative charges that could interact with the pesticide, but many of these negatively charged sites would be compromised by the presence of calcium involved in the bead synthesis.

In order to check if pH produced changes in PQ adsorption, additional isotherms were performed onto A-MMT70 at pH 4 and 11 (Supplementary material). No changes were observed. PQ is a quaternary ammonium cation and, as most of this kind of molecules, has permanent positive charge independently of the pH of its solution. In addition, montmorillonite keeps its negative charge in this pH range (see below). These properties explain why pH does not affect PQ adsorption.

The zeta potential experiments showed that sodium alginate, montmorillonite, A-MMT0 and A-MMT70 beads maintain their negative charge in a wide pH range from 4 to 9 (Supplementary material). These experiments showed that A-MMT0 beads have a lower negative charge than pure sodium alginate at all pH measured. This decrease may be due to the presence of calcium ions in the bead. The negative charge at constant pH is also maintained for the beads after PQ adsorption. These results agree with data showed by de Keizer [65] for PQ adsorbed onto pure montmorillonite. The facts that pH did not change with adsorption, that adsorption did not change with pH, and that zeta potential did not change either are in agreement with an ion exchange mechanism as reported by other authors [65,66].

It is important to know to what extent each of the beads components is responsible for the PQ adsorption. Therefore, the following equations are proposed where it is assumed that both the alginate and the MMT adsorb the pesticide in an independent way without being affected by each other's presence. If this is the case the following equation holds:

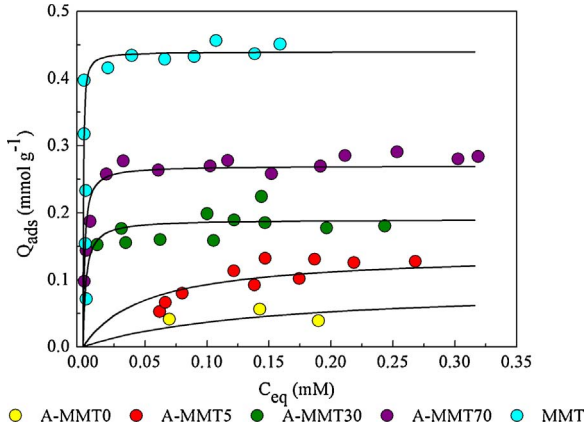

Fig. 7. Adsorption isotherm of PQ onto the beads (A-MMT0; A-MMT5; A-MMT30 and A-MMT-70) and the MMT suspension.

Table 3
Langmuir isotherm parameters (K_L and Q_{max}) of PQ adsorption onto the beads.

Sample	Q_{max} (mmol g^{-1}) Calculated[a]	Q_{max} (mmol g^{-1})	K_L (L $mmol^{-1}$)	R^2
A-MMT0	0.102	0.093	7.58	0.766
A-MMT5	0.121	0.146	16.68	0.859
A-MMT30	0.196	0.187	301.29	0.871
A-MMT70	0.321	0.278	979.25	0.987
MMT	0.415	0.442	1399	0.520

[a] Values calculated with Eq. (7): straight line with y-axis intercept 0.1021 mmol g^{-1} and slope 0.313 mmol g^{-1}.

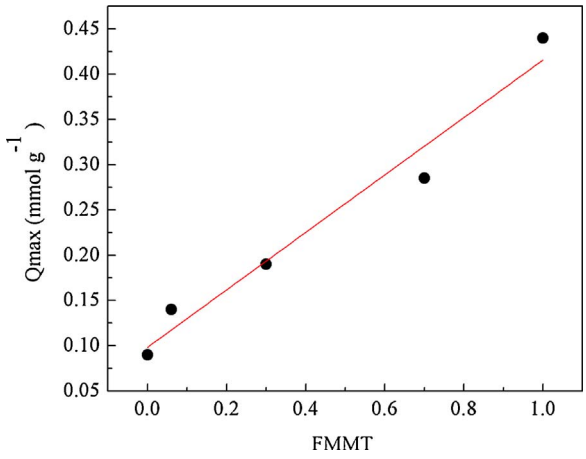

Fig. 8. Maximum amount of PQ adsorbed in mmol g^{-1} (Qmax) vs grams of MMT per gram of bead (FMMT).

$$Q_{max} = Q_{max(ALG)}F_{ALG} + Q_{max(MMT)}F_{MMT} \quad (3)$$

where $Q_{max(ALG)}$ (mmol g^{-1}) is the maximum amount of PQ adsorbed on a pure alginate bead and $Q_{max(MMT)}$ (mmol g^{-1}) is the maximum amount of PQ adsorbed on pure MMT. In addition F_{ALG} and F_{MMT} are given by:

$$F_{ALG} = m_{ALG}/m_{bead} \quad (4)$$

$$F_{MMT} = m_{MMT}/m_{bead} \quad (5)$$

$$F_{ALG} + F_{MMT} = 1 \quad (6)$$

where m_{ALG} and m_{MMT} are the mass in grams of alginate and MMT respectively in the beads.

Combining Eqs. (3) and (6) the following equation is obtained:

$$Q_{max} = Q_{max(ALG)} + (Q_{max(MMT)} - Q_{max(ALG)})F_{MMT} \quad (7)$$

Eq. (7) shows that a plot Q_{max} vs. F_{MMT} should result in a straight line, with an expected y-axis intercept equal to $Q_{max(ALG)} = 0.093$ mmol g^{-1} and an expected slope equal to $(Q_{max(MMT)} - Q_{max(ALG)}) = 0.349$ mmol g^{-1}. Fig. 8 depicts such a plot, and the y-axis intercept and slope obtained from least square fitting were respectively (0.1021 ± 0.016) mmol g^{-1} and a slope (0.313 ± 0.033), showing a good agreement with the expected parameters and indicating that alginate and montmorillonite adsorb PQ in an independent way in the beads. In addition, a comparison of Q_{max} and K_L values for pure alginate (sample A-MMT0) with the corresponding values for pure MMT (see Table 3) shows that alginate is a much poorer and weaker PQ adsorbent. Therefore, the main role of MMT in the beads is to act as the PQ adsorbent, whereas the polymer plays a very important role as support of the clay particles allowing for an effortless handling of the particles with the adsorbed pollutant.

There is no information in the literature about PQ adsorption on this kind of materials to make a comparison of the results obtained. Rytwo et al. [67] present an adsorption study of different organocations with delocalized charge, such as paraquat, diquat, methyl blue and metyl green onto sepiolite. The adsorption was similar at low concentrations. For that, one might think that other positively charged organic molecules such as methylene blue (MB) and crystal violet (CV) may have similar behaviour when adsorbing on alginate-clay beads, but the literature shows that this comparison is not so straightforward. Indeed, there are articles in which the alginate-clay beads are better adsorbents of the dye than pure clay [37], and others where alginate beads without clay are shown to be good adsorbents, but there was not comparing with the behaviour on clays [36]. Cavallaro et al. [35], working with CV on alginate-halloysite beads, showed that the adsorption of the dye increased with increasing halloysite content, in agreement with what we found here with PQ, although they did not find a linear relationship. This indicates that it is necessary to further explore the adsorption of cationic herbicides on clay-alginate materials.

4. Conclusions

In the present work alginate-montmorillonite beads were prepared with different. They were characterized and evaluated by their capacity to remove the herbicide PQ from aqueous solutions. The adsorbed amount of PQ was linearly dependent on the montmorillonite content. MMT is the main adsorbent of PQ in the beads. Although alginate is a much poorer adsorbent than MMT, it plays a very important role as support of the clay particles. The prepared materials are easier to handle and can be easily separated from the reaction media. The experimental data obtained from this work shows that alginate-montmorillonite beads are efficient materials to adsorb cationic pesticides as PQ from aqueous solutions. These beads have a high potential to be used for water purification.

Acknowledgments

The authors of this work acknowledge CONICET and UNS for the financial support. Language assistance by native English speaker Dave Lovell is gratefully acknowledged. The authors thank Fernando Cappa for performing the digital photographs.

Appendix A. Supplementary data

Supplementary data associated with this article can be found, in the online version, at https://doi.org/10.1016/j.jece.2017.11.018.

References

[1] D. Pimentel, Amounts of pesticides reaching target pests: environmental impacts and ethics, J. Agric. Environ. Ethics 8 (1995) 17–29.
[2] R.H. Bromilow, Paraquat and sustainable agriculture, Pest Manag. Sci. 60 (2004) 340–349.
[3] F. He, P. Xu, J. Zhang, Q. Zhang, S. Gu, Y. Liu, J. Wang, Efficacy and safety of pulse immunosuppressive therapy with glucocorticoid and cyclophosphamide in patients with paraquat poisoning: a meta-analysis, Int. Immunopharmacol. 27 (2015) 1–7.
[4] M.F. Charão, M. Baierle, B. Gauer, G. Goethel, R. Fracasso, K. Paese, N. Brucker, A.M. Moro, G.B. Bubols, B.B. Dias, U.S. Matte, S.S. Guterres, A.R. Pohlmann, S.C. Garcia, Protective effects of melatonin-loaded lipid-core nanocapsules on paraquat-induced cytotoxicity and genotoxicity in a pulmonary cell line, Mutat. Res. Genet. Toxicol. Environ. Mutagen. 784–785 (2015) 1–9.
[5] C.L. Szemruch, S.J. Renteria, F. Moreira, M.A. Cantamutto, L. Ferrari, D.P. Rondanini, Germination, vigour and dormancy of sunflower seeds following chemical desiccation of female plants, Seed Sci. Technol. 42 (2014) 454–460.
[6] Paraquat Information Center, Paraquat Herbicide for Non-Selective Weed Control in No-Till and Other Sustainable Agriculture Systems, (2016) (Accessed February 17, 2017), http://paraquat.com/.
[7] S. Walker, L. Boucher, T. Cook, B. Davidson, A. McLean, M. Widderick, Weed age affects chemical control of Conyza bonariensis in fallows, Crop Prot. 38 (2012) 15–20.
[8] B.S. Ismail, M. Sameni, M. Halimah, Evaluation of herbicide pollution in the kerian ricefields of Perak, Malaysia, World Appl. Sci. J. 15 (2011) 05–13.
[9] EPA, Unites States Environmental Protection Agency, Paraquat and Diquat, (2005).
[10] A. Kyoungjin, J. Guo, E. Lee, S. Jeong, Y. Zhao, Z. Wang, T. Leiknes, PDMS/PVDF hybrid electrospun membrane with superhydrophobic property and drop impact dynamics for dyeing wastewater treatment using membrane distillation, J. Memb. Sci. 525 (2017) 57–67.
[11] K. Raghava, K.V. Karthik, S.B.B. Prasad, S.K. Soni, H.M. Jeong, A.V. Raghu, Enhanced photocatalytic activity of nanostructured titanium dioxide/polyaniline hybrid photocatalysts, Polyhedron 120 (2016) 169–174.
[12] P. Liu, L. Zhang, Adsorption of dyes from aqueous solutions or suspensions with clay nano-adsorbents, Sep. Purif. Technol. 58 (2007) 32–39.
[13] J.M. Dias, M.C.M. Alvim-Ferraz, M.F. Almeida, J. Rivera-Utrilla, M. Sánchez-Polo, Waste materials for activated carbon preparation and its use in aqueous-phase treatment: a review, J. Environ. Manage. 85 (2007) 833–846.
[14] N.K. Lazaridis, G.Z. Kyzas, A.A. Vassiliou, D.N. Bikiaris, Chitosan derivatives as biosorbents for basic dyes, Langmuir 23 (2007) 7634–7643.
[15] S. Mondal, Methods of dye removal from dye house effluent—an overview, Environ. Eng. Sci. 25 (2008) 383–396.
[16] G. Crini, Recent developments in polysaccharide-based materials used as adsorbents in wastewater treatment, Prog. Polym. Sci. 30 (2005) 38–70.
[17] G. Crini, Non-conventional low-cost adsorbents for dye removal: a review, Bioresour. Technol. 97 (2006) 1061–1085.

[18] F. Delval, G. Crini, S. Bertini, C. Filiatre, G. Torri, Preparation, characterization and sorption properties of crosslinked starch-based exchangers, Carbohydr. Polym. 60 (2005) 67–75.
[19] G. Bayramoglu, A. Denizli, S. Bektas, M.Y. Arica, Entrapment of Lentinus sajor-caju into Ca-alginate gel beads for removal of Cd(II) ions from aqueous solution: preparation and biosorption kinetics analysis, Microchem. J. 72 (2002) 63–76.
[20] C. Ribeiro, C. Barrias, M. Barbosa, Calcium phosphate-alginate microspheres as enzyme delivery matrices, Biomaterials 25 (2004) 4363–4373.
[21] O. Smidsrød, G. Skjåk-Braek, Alginate as immobilization matrix for cells, Trends Biotechnol. 8 (1990) 71–78.
[22] R. Aravindhan, N.N. Fathima, J.R. Rao, B.U. Nair, Equilibrium and thermodynamic studies on the removal of basic black dye using calcium alginate beads, Colloids Surf. A Physicochem. Eng. Asp. 299 (2007) 232–238.
[23] M.F. Nasr, S.M. Abo El-Ola, A. Ramadan, A. Hashem, A comparative study between the adsorption behavior of activated carbon fiber and modified alginate I. Basic dyes adsorption, Polym. Plast. Technol. Eng. 45 (2006) 335–340.
[24] V. Rocher, J.-M. Siaugue, V. Cabuil, A. Bee, Removal of organic dyes by magnetic alginate beads, Water Res. 42 (2008) 1290–1298.
[25] R.M.P. Silva, J.P.H. Manso, J.R.C. Rodrigues, R.J.L. Lagoa, A comparative study of alginate beads and an ion-exchange resin for the removal of heavy metals from a metal plating effluent, J. Environ. Sci. Heal. Part A 43 (2008) 1311–1317.
[26] S. Kittinaovarat, P. Kansomwan, N. Jiratumnukul, Chitosan/modified montmorillonite beads and adsorption reactive red 120, Appl. Clay Sci. 48 (2010) 87–91.
[27] Y. Tal, J. van Rijn, A. Nussinovitch, Improvement of structural and mechanical properties of denitrifying alginate beads by Freeze-Drying, Biotechnol. Prog. 13 (1997) 788–793.
[28] L. Yu, K. Dean, L. Li, Polymer blends and composites from renewable resources, Prog. Polym. Sci. 31 (2006) 576–602.
[29] R.S. Varma, Clay and clay-supported reagents in organic synthesis, Tetrahedron 58 (2002) 1235–1255.
[30] G.W. Bailey, J.L. White, T. Rothberg, Adsorption of organic herbicides by montmorillonite, Soil Sci. Soc. Am. Pro. 32 (1968) 222–234.
[31] N. Shrimp, R.A. Griffin, Attenuation of Pollutants in Municipal Landfill Leachate by Clay Minerals, (1976) Final Report for U.S Environmental Protection Agency Contract, No 68-03-0211. Cincinnati, OH.
[32] E. Montarges, A. Moreau, L.J. Michot, Removing of organic toxicants from water by Al –pluronic modified clay, Appl. Clay Sci. 13 (1998) 165–185.
[33] R. Ilari, M. Etcheverry, C. Zenobi, G. Zanini, Effect of the surfactant benzalkonium chloride in the sorption of paraquat and cadmium on montmorillonite, Int. J. Environ. Health 7 (2014) 70–82.
[34] A. Itadani, M. Tanaka, T. Abe, H. Taguchi, M. Nagao, Al-pillared montmorillonite clay minerals: low-pressure CO adsorption at room temperature, J. Colloid Interface Sci. 313 (2007) 747–750.
[35] G. Cavallaro, A. Gianguzza, G. Lazzara, S. Milioto, D. Piazzese, Alginate gel beads filled with halloysite nanotubes, Appl. Clay Sci. 72 (2013) 132–137.
[36] A.F. Hassan, A.M. Abdel-Mohsen, M.M.G. Fouda, Comparative study of calcium alginate activated carbon, and their composite beads on methylene blue adsorption, Carbohydr. Polym. 102 (2014) 192–198.
[37] A.A. Oladipo, M. Gazi, Enhanced removal of crystal violet by low cost alginate/acid activated bentonite composite beads: optimization and modelling using non-linear regression technique, J. Water Process Eng. 2 (2014) 43–52.
[38] A. Benhouria, M.A. Islam, H. Zaghouane-Boudiaf, M. Boutahala, B.H. Hameed, Calcium alginate-bentonite-activated carbon composite beads as highly effective adsorbent for methylene blue, Chem. Eng. J. 270 (2015) 621–630.
[39] B. Singh, D.K. Sharma, R. Kumar, A. Gupta, Controlled release of the fungicide thiram from starch-alginate-clay based formulation, Appl. Clay Sci. 45 (2009) 76–82.
[40] B. Singh, D.K. Sharma, R. Kumar, A. Gupta, Controlled release of thiram from neem-alginate-clay based delivery systems to manage environmental and health hazards, Appl. Clay Sci. 47 (2010) 384–391.
[41] G. Rytwo, S. Nir, L. Margulies, A model for adsorption of divalent organic cations to montmorillonite, J. Colloid Interface Sci. 560 (1996) 551–560.
[42] G. Rytwo, S. Nir, L. Margulies, Adsorption and interactions of diquat and paraquat with montmorillonite, Soil Sci. Soc. Am. J. 60 (1996) 601.
[43] M.H. Gorakhki, C.A. Bareither, Salinity effects on sedimentation behavior of kaolin bentonite, and soda ash mine tailings, Appl. Clay Sci. 114 (2015) 593–602.
[44] W.D. Keller, R.C. Reynolds, A. Inoue, Morphology of clay minerals in the smectite-to illite conversion series by scanning electron microscopy, Clays Clay Miner. 34 (1986) 187–197.
[45] A. Rashidzadeh, A. Olad, M.J. Hejazi, Controlled release systems based on intercalated paraquat onto montmorillonite and clinoptilolite clays encapsulated with sodium alginate, Adv. Polym. Technol. 36 (2017) 177–185.
[46] G.P. Zanini, R.G. Ovesen, H.C.B. Hansen, B.W. Strobel, Adsorption of the disinfectant benzalkonium chloride on montmorillonite. Synergistic effect in mixture of molecules with different chain lengths, J. Environ. Manage. 128 (2013) 100–105.
[47] G. Sen, S.R. Prakash, S. Pal, Microwave-initiated synthesis of polyacrylamide grafted sodium alginate: synthesis and characterization, J. Appl. Polym. Sci. 115 (2010) 63–71.
[48] G. Lawrie, I. Keen, B. Drew, A. Chandler-Temple, L. Rintoul, A. Peter Fredericks, Lisbeth Grøndahl, Interactions between alginate and chitosan biopolymers characterized using FTIR and XPS, Biomacromolecules 8 (2007) 2533–2541.
[49] W. Yang, L. Zhang, L. Wu, J. Li, J. Wang, H. Jiang, Y. Li, Synthesis and characterization of MMA-NaAlg/hydroxyapatite composite and the interface analyse with molecular dynamics, Carbohydr. Polym. 77 (2009) 331–337.
[50] Y.-N. Daia, P. Lia, J.-P. Zhang, A.-Q. Wang, Q. Wei, A novel pH sensitive N-succinyl chitosan/alginate hydrogel bead for nifedipine delivery, Biopharm. Drug Dispos. 29 (2008) 173–184.
[51] J.T. Kloprogge, Spectroscopic studies of synthetic and natural beidellites: a review, Appl. Clay Sci. 31 (2006) 165–179.
[52] C. Bertagnolli, M.G.C. da Silva, Characterization of Brazilian bentonite organoclays as sorbents of petroleum-derived fuels, Mater. Res. 15 (2012) 253–259.
[53] D. Ait Sidhoum, M. Socías-Viciana, A. Derdour, E. González-Pradas, N. Debbagh-Boutarbouch, Removal of paraquat from water by an Algerian bentonite, Appl. Clay Sci. 83–84 (2013) 441–448.
[54] T. Jiang, Q. Zhao, H. Yin, Synthesis of highly stabilized mesoporous molecular sieves using natural clay as raw material, Appl. Clay Sci. 35 (2007) 155–161.
[55] W. Gates, J. Anderson, G. Churchman, Mineralogy of a bentonite from Miles Queensland, Australia and characterisation of its acid activation products, Appl. Clay Sci. 20 (2002) 189–197.
[56] J. Madejová, J. Bujdák, M. Janek, P. Komadel, Comparative FT-IR study of structural modifications during acid treatment of dioctahedral smectites and hectorite, Spectrochim. Acta Part A Mol. Biomol. Spectrosc. 54 (1998) 1397–1406.
[57] P. Praus, M. Turicová, S. Študentová, M. Ritz, Study of cetyltrimethylammonium and cetylpyridinium adsorption on montmorillonite, J. Colloid Interface Sci. 304 (2006) 29–36.
[58] P. Laurienzo, M. Malinconico, A. Motta, A. Vicinanza, Synthesis and characterization of a novel alginate–poly (ethylene glycol) graft copolymer, Carbohydr. Polym. 62 (2005) 274–282.
[59] A. Parikh, D. Madamwar, Partial characterization of extracellular polysaccharides from cyanobacteria, Bioresour. Technol. 97 (2006) 1822–1827.
[60] A.A. Said, R.M. Hassan, Thermal decomposition of some divalent metal alginate gel compounds, Polym. Degrad. Stab. 39 (1993) 393–397.
[61] A. Said, M. Abd El-Wahab, R. Hassan, Thermal and electrical studies on some metal alginate compounds, Thermochim. Acta 233 (1994) 13–24.
[62] J.P. Soares, J.E. Santos, G.O. Chierice, E.T.G. Cavalheiro, Thermal behavior of alginic acid and its sodium salt, Ecl. Quim. 29 (2004) 53.
[63] M. Földvári, Handbook of the Thermogravimetric System of Minerals and Its Use in Geological Practice 213 Geol. Inst., Hungary, 2011, pp. 76–78.
[64] W.D. Keller, Clay Minerals of the Morrison Formation of the Colorado Plateau, Geological Survey Bulletin 1150, U.S. Goverment, Washington, 1962, pp. 12–13.
[65] A. de Keizer, Adsorption of paraquat ions on clay minerals. Electrophoresis of clay particles, Progr. Colloid Polym. Sci. 126 (1990) 118–126.
[66] G.H. Bolt, M.F. De Boodt, M.H.B. Hayes, M.B. McBride (Eds.), Interactions at the Soil Colloid-Soil Solution Interface, Springer-Science, Belgium, 1986.
[67] G. Rytwo, D. Tropp, C. Serban, Adsorption of diquat, paraquat and methyl green on sepiolite: experimental results and model calculations, Appl. Clay Sci. 20 (2002) 273–282.